Supplementary Material (ESI) for Photochemical & Photobiological Sciences

ELECTRONIC SUPPLEMENTARY INFORMATION

BICARBONATE-ENHANCED TRANSFORMATION OF PHENOL UPON IRRADIATION OF HEMATITE, NITRATE, AND NITRITE

Serge Chiron,[a] Stéphane Barbati,[a] Swapan Khanra,[b,c] Binay K. Dutta,[b,d] Marco Minella,[c] Claudio Minero,[c] Valter Maurino,[c] Ezio Pelizzetti,[c] Davide Vione[c,*]

[a] *Laboratoire Chimie Provence, Aix-Marseille Universités-CNRS (UMR 6264), 3 place Victor Hugo, 13331 Marseille cedex 3, France.*

[b] *Department of Chemical Engineering, University of Calcutta, 92 Acharya Prafulla Chandra Road, 700009 Kolkata, India.*

[c] *Dipartimento di Chimica Analitica, Università di Torino, Via Pietro Giuria 5, 10125 Torino, Italy. http://www.chimicadellambiente.unito.it*

[d] *Chemical Engineering Department, University of Technology Petronas, 31750 Tronoh, Perak Darul Ridzuan, Malaysia.*

* Corresponding author. Phone +39-011-6707633; Fax +39-011-6707615; E-mail: *davide.vione@unito.it*
URL: *http://naturali.campusnet.unito.it/cgi.bin/docenti.pl/Show?_id=vione*

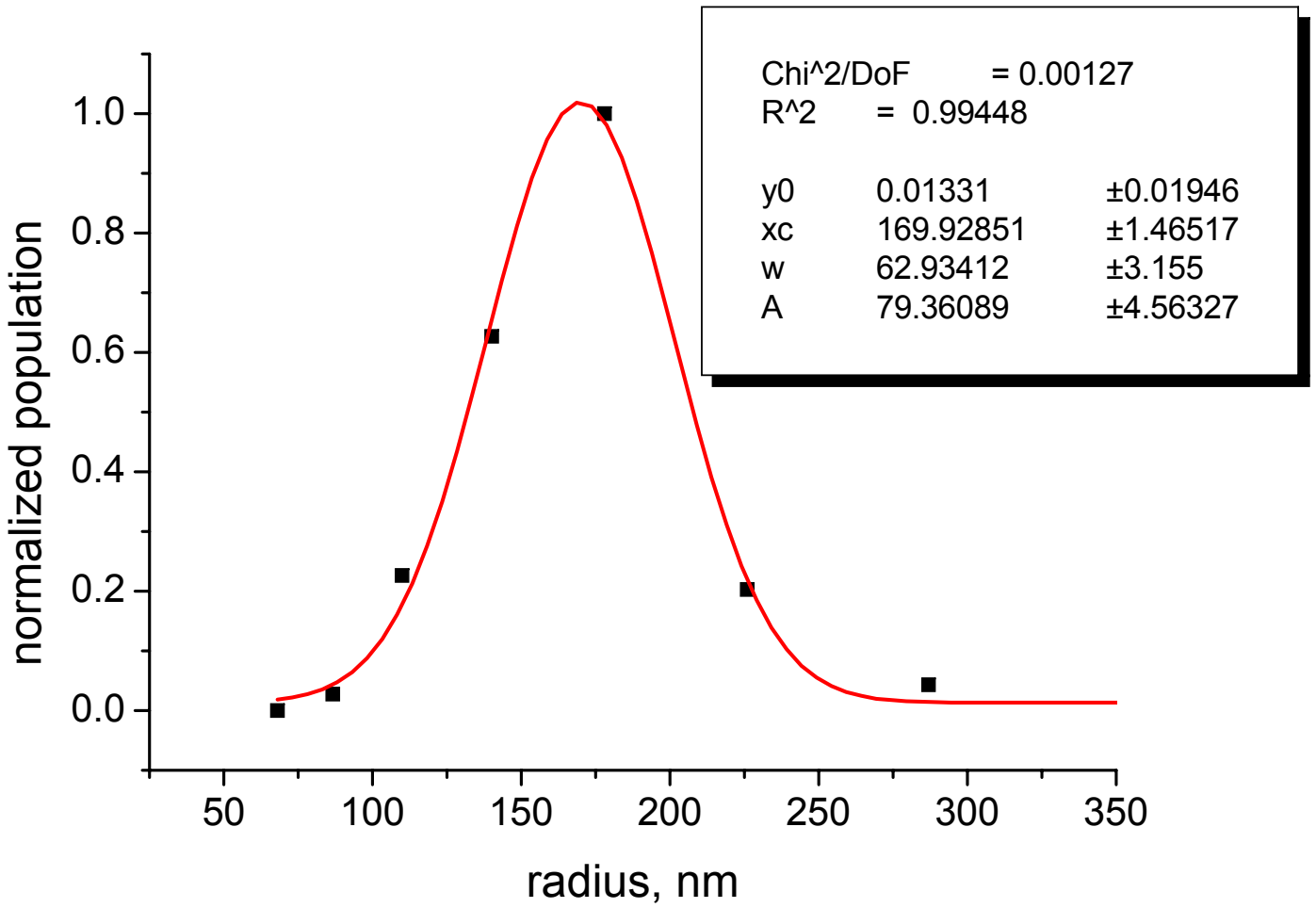

Figure S1. Radius distribution of the hematite particles adopted in the present work.

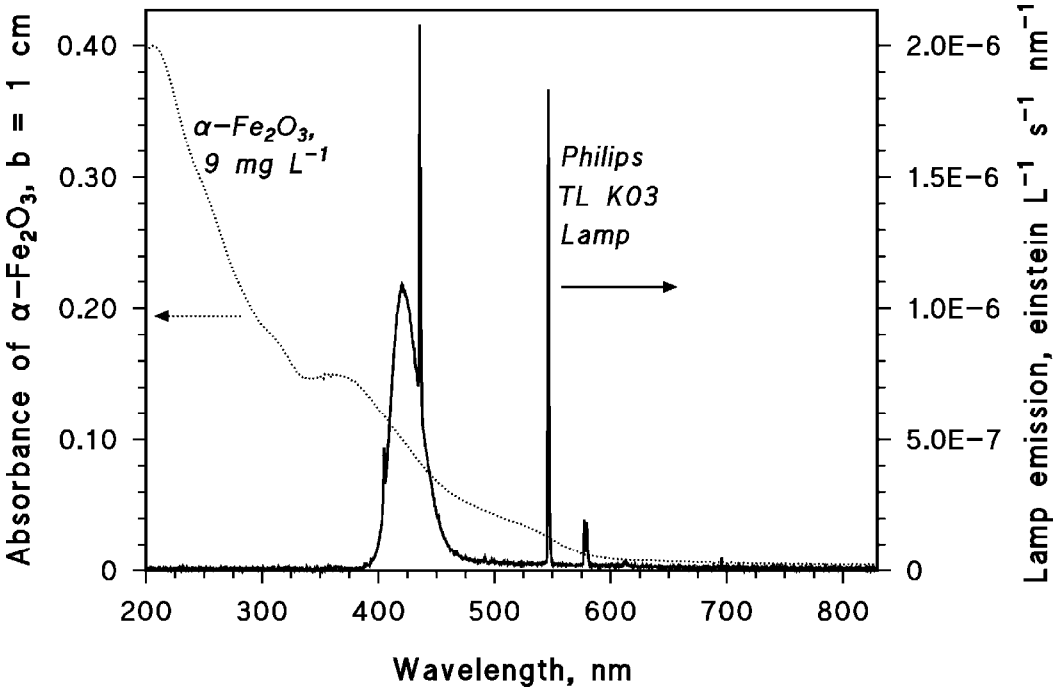

Figure S2. Absorbance of 9 mg L^{-1} hematite (optical path length b = 1 cm) and emission spectrum of the adopted blue lamp.

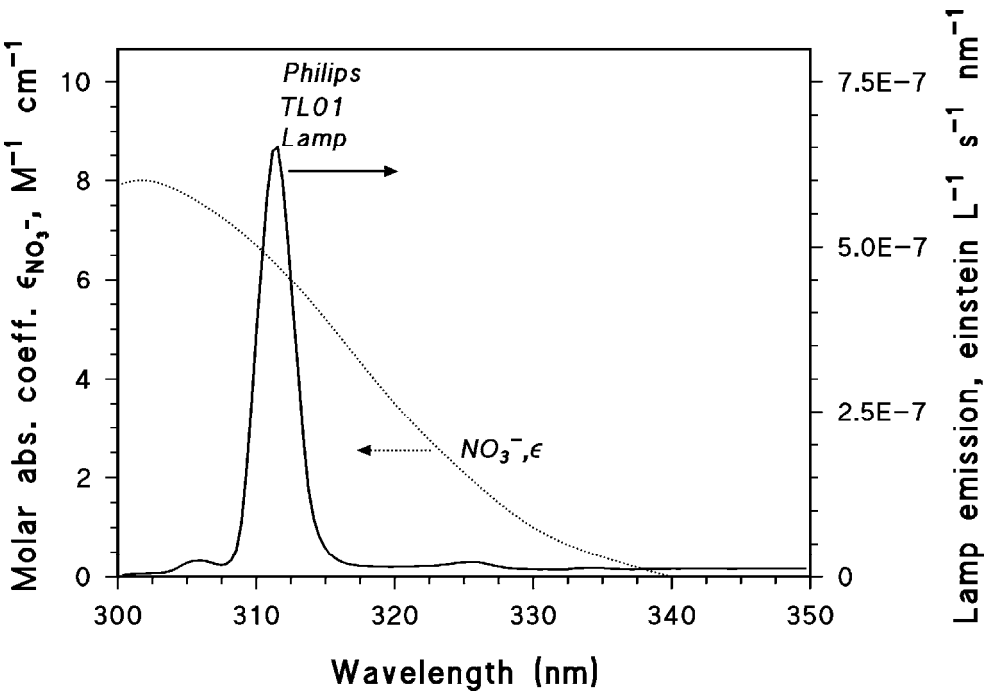

Figure S3. Absorption spectrum of nitrate and emission spectrum of the adopted UVB lamp.

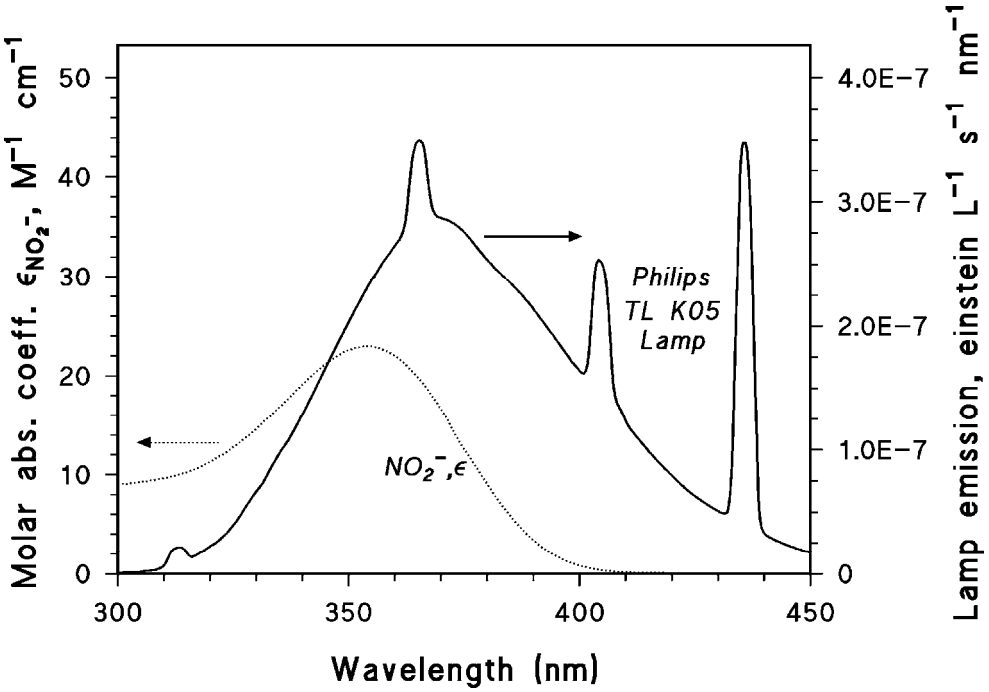

Figure S4. Absorption spectrum of nitrite and emission spectrum of the adopted UVA lamp.

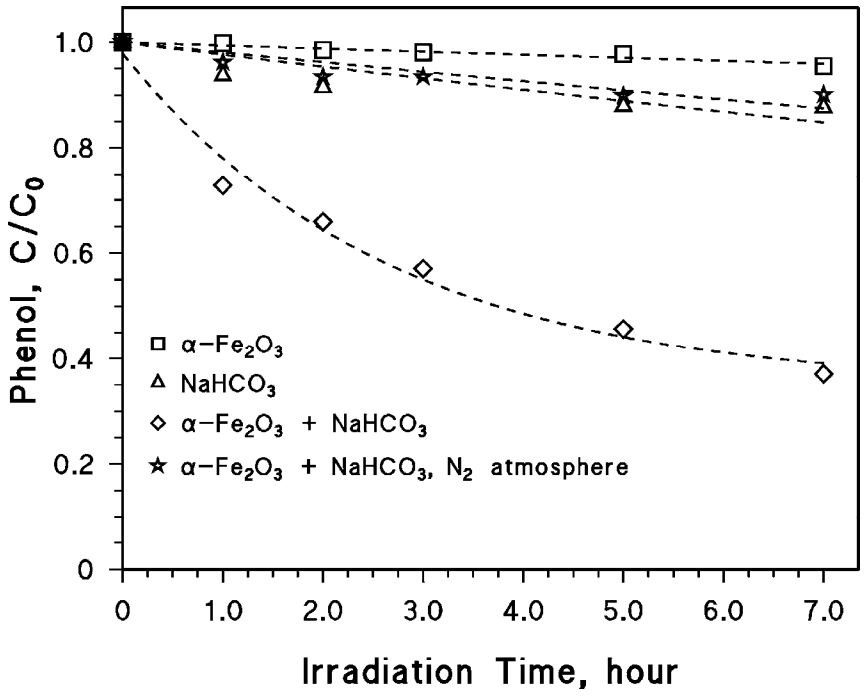

Figure S5. Time evolution of phenol (C_0 = 25 μM) upon irradiation under blue light (Philips TL K03 lamp) of 450 mg L^{-1} α-Fe_2O_3 and/or 10 mM $NaHCO_3$, in aerated solution and under N_2 atmosphere.

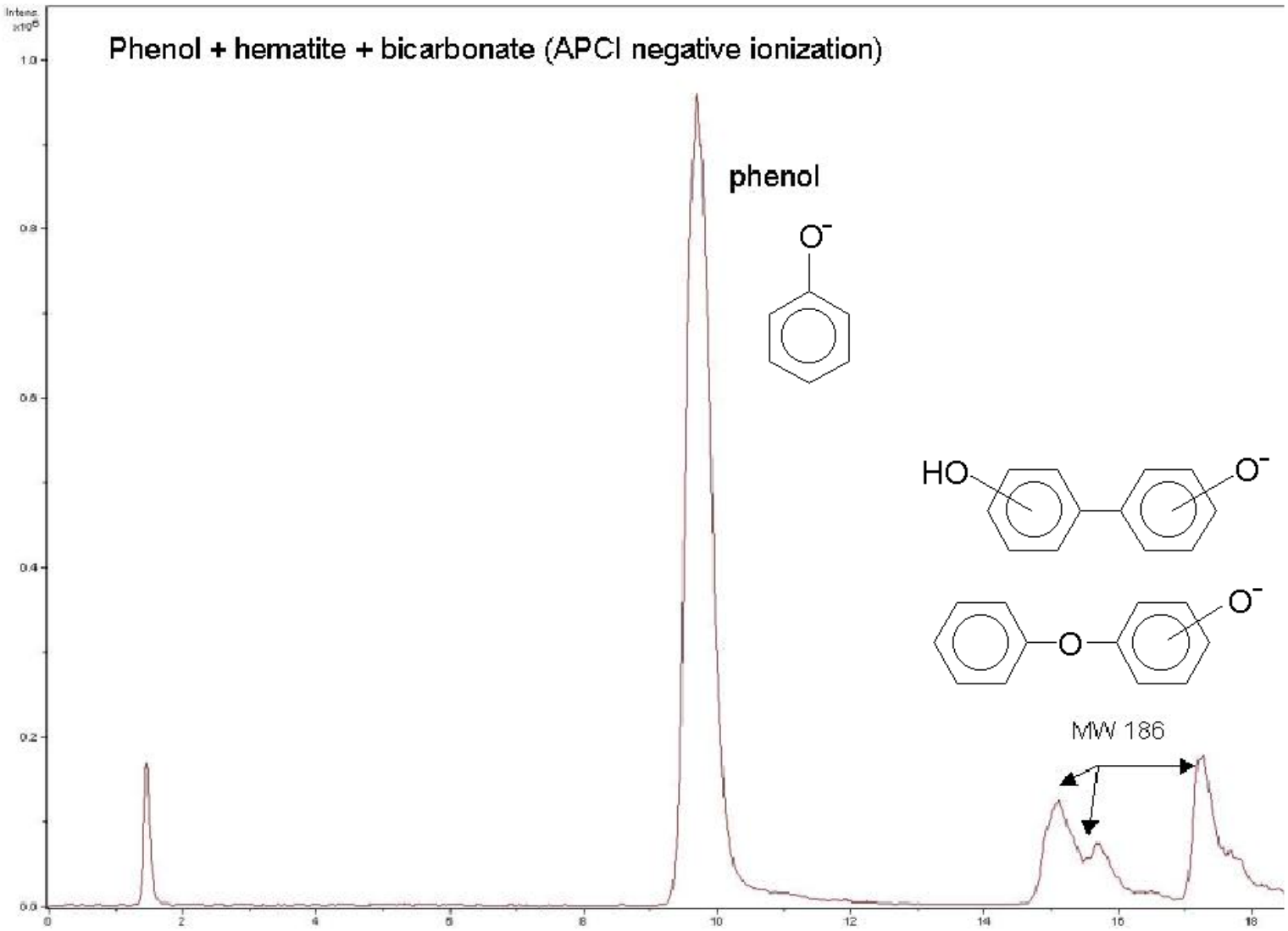

Figure S6. HPLC-APCI-MS chromatogram of the phenol + hematite + bicarbonate system under irradiation.

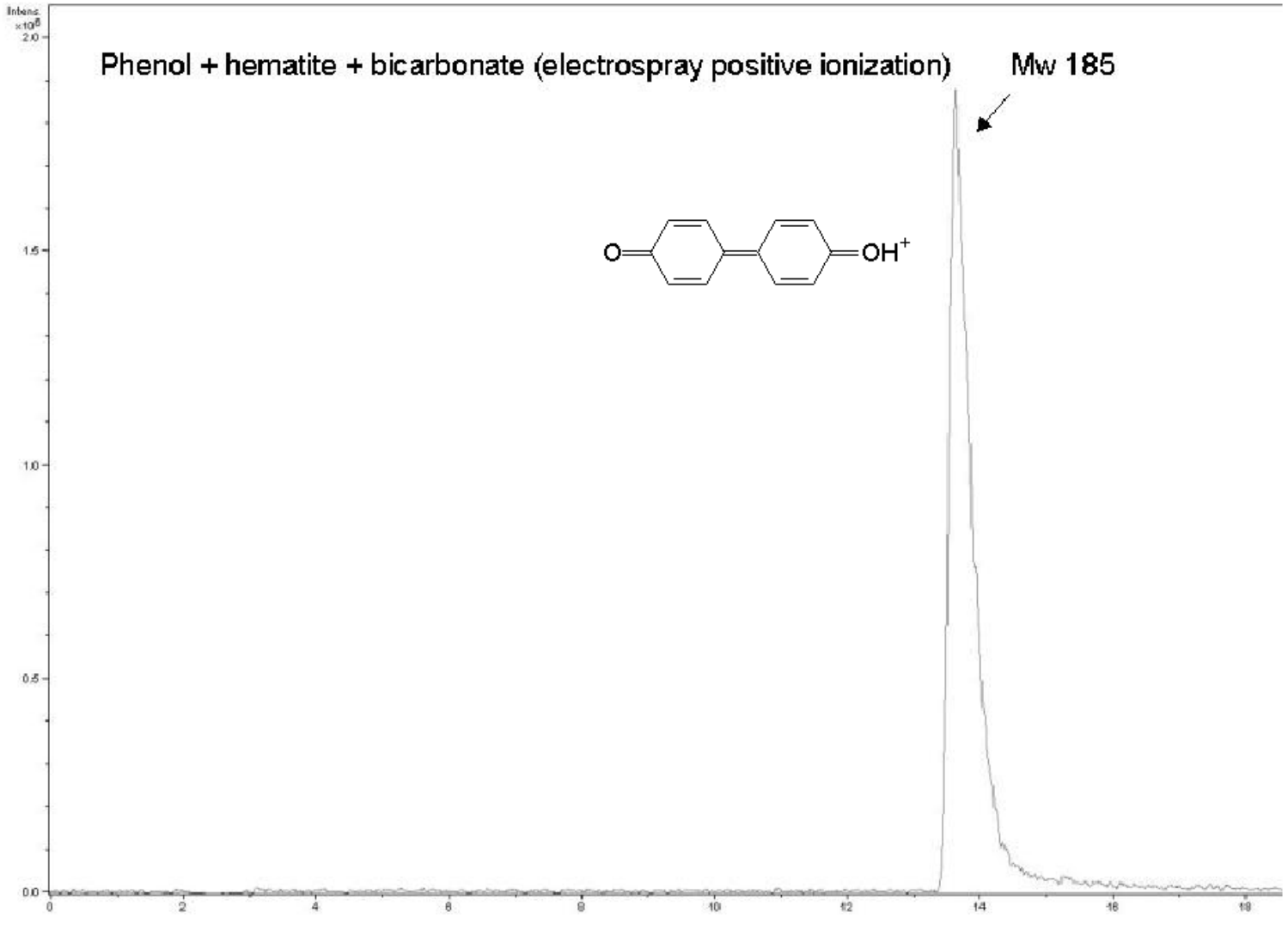

Figure S7. HPLC-ESP-MS chromatogram of the phenol + hematite + bicarbonate system under irradiation.

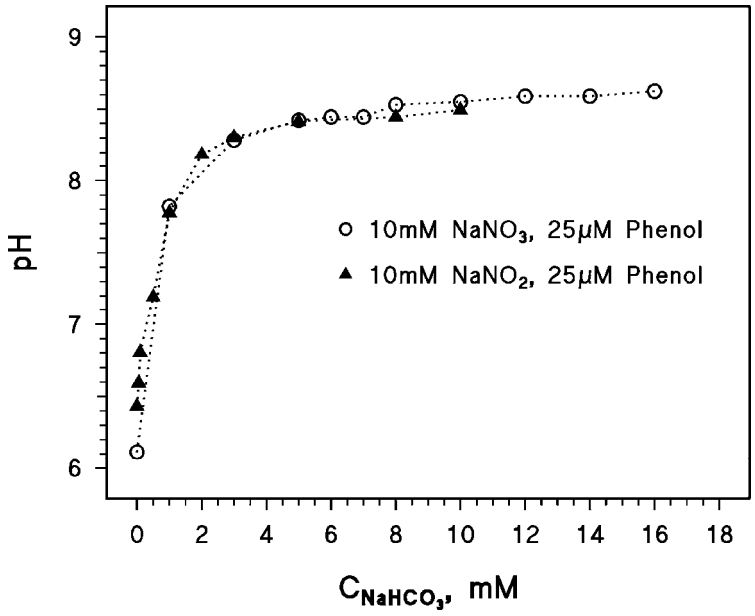

Figure S8. pH trend with bicarbonate of the solutions containing 25 μM phenol and 10 mM $NaNO_2$ or $NaNO_3$.

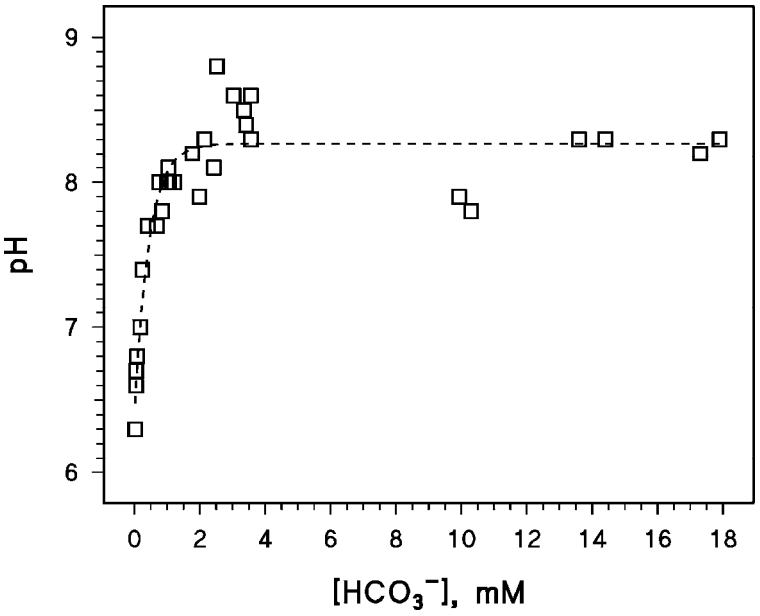

Figure S9. pH trend of natural water samples as a function of the concentration of bicarbonate (*1*,*2*,*3*). To be compared with Figure S8.

1) D. Vione, G. Falletti, V. Maurino, C. Minero, E. Pelizzetti, M. Malandrino, R. Ajassa, R. I. Olariu, C. Arsene, Sources and sinks of hydroxyl radicals upon irradiation of natural waters samples, *Environ. Sci. Technol.* 2006, **40**, 3775-3781.

2) C. Minero, S. Chiron, G. Falletti, V. Maurino, E. Pelizzetti, R. Ajassa, M. E. Carlotti, D. Vione, Photochemical processes involving nitrite in surface water samples, *Aquat. Sci.* 2007, **69**, 71-85.

3) C. Minero, V. Lauri, V. Maurino, E. Pelizzetti, D. Vione, A model to predict the steady-state concentration of hydroxyl radicals in the surface layer of natural waters, *Ann. Chim. (Rome)*, 2007, **97**, 685-698.

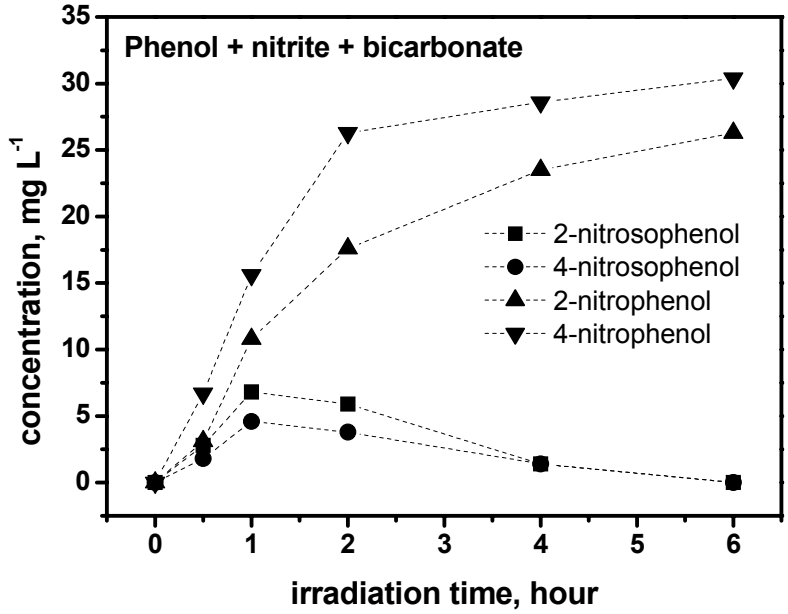

Figure S10. Time evolution of the nitro- and nitrosophenols upon irradiation of 25 μM phenol + 10 mM $NaNO_2$ + 5 mM phosphate buffer.

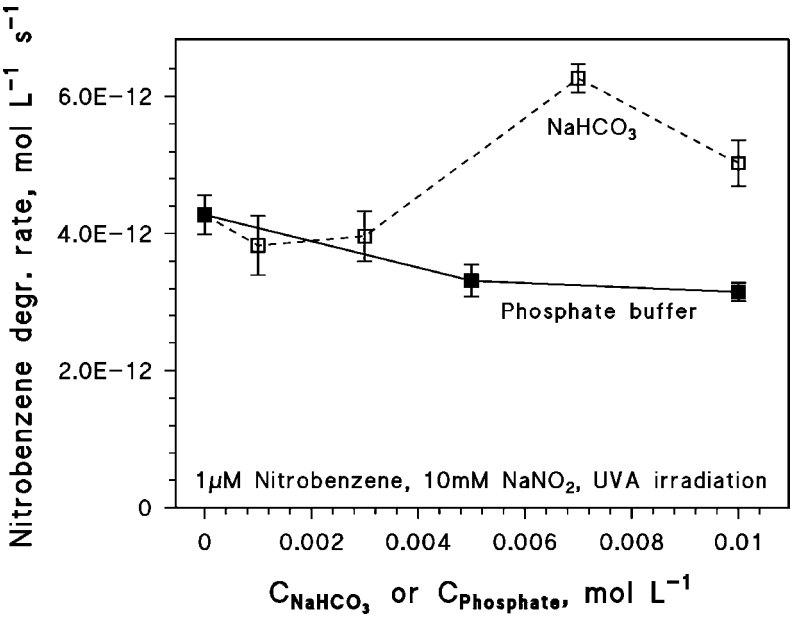

Figure S11. Initial degradation rate of 1 μM nitrobenzene upon UVA irradiation of 10 mM $NaNO_2$, as a function of the concentration of $NaHCO_3$ or the phosphate buffer (NaH_2PO_4 + Na_2HPO_4).

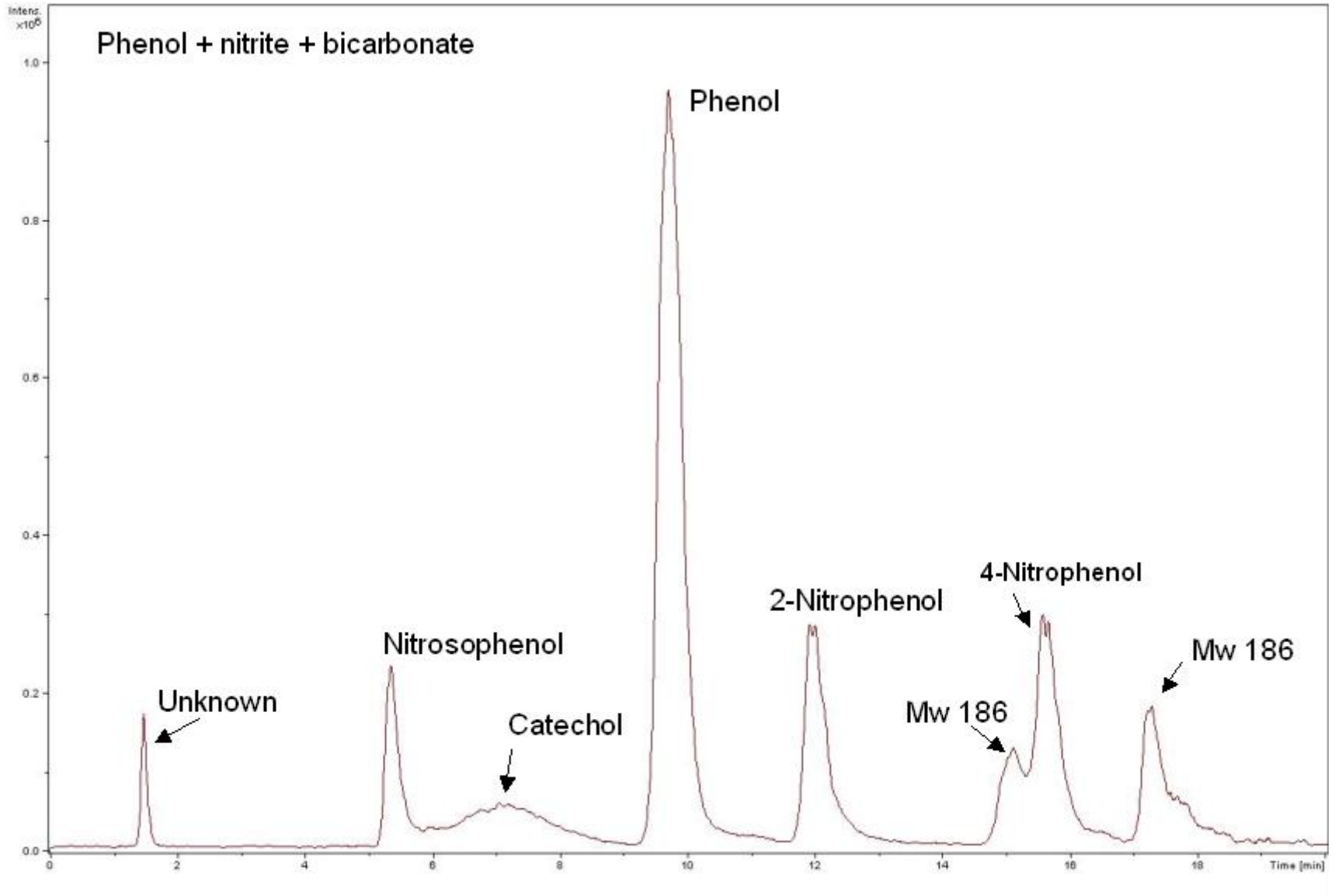

Figure S12. HPLC-APCI-MS chromatogram of the phenol + nitrite + bicarbonate system under irradiation.

MODELLING PHENOL TRANSFORMATION AND NITROPHENOL FORMATION IN THE PRESENCE OF NITRITE AND BICARBONATE UNDER IRRADIATION

The following Figures (S13-S15) show the trend of the initial rates of phenol transformation and nitrophenol formation upon irradiation of nitrite and bicarbonate, as a function of the initial concentrations of nitrite and phenol. The corresponding trend as a function of the concentration of bicarbonate is reported as Figure 3 in the manuscript. Here the focus will be on the effects of phenol and nitrite on the formation rate of nitrophenols.

The trend of the rates with [Phenol] suggests a saturation effect at the highest adopted concentration values (Figure S13). However, aromatic pollutants in surface waters (and phenol makes no exception) are expected to reach lower values and therefore the rate of nitrophenol formation would be directly proportional to [Phenol]. Accordingly, it is possible to consider the tangent at [Phenol] = 0 to the curve fitting the experimental data (which is of the form $y = a\,x\,(x + b)^{-1}$), as shown in Figure S13.

The increase of the rates with $[NO_2^-]$ (Figure S14) would mainly be accounted for by the increasing absorption of radiation with increasing nitrite, because the photolysis of NO_2^- is the driving force of the process. To allow the application of the model to different irradiation conditions than those adopted in the present work, consideration of the nitrite effect was based on the radiation absorption flux, $I_{abs}^{NO_2^-} = \int_{\lambda} I_0(\lambda) \cdot \left(1 - 10^{-\varepsilon(\lambda) \cdot b \cdot [NO_2^-]}\right) d\lambda$. The quantity $\varepsilon(\lambda)$ is the molar absorption coefficient of nitrite, b = 0.4 cm is optical path length of the solution, and $[NO_2^-]$ is in molarity. $I_0(\lambda)$ is the spectral photon flux density of the lamp in einstein L^{-1} s^{-1} nm^{-1} (see Figure S4), and it is $\int_{\lambda} I_0(\lambda) d\lambda = 2.2 \cdot 10^{-5}$ einstein L^{-1} s^{-1}. The experimental data show a good linear dependence of the initial formation rates of nitrophenols as a function of $I_{abs}^{NO_2^-}$ (Figure S15).

From the data of Figure 13 (tangents at [Phenol] = 0) and those of Figure 15 it is possible to derive the dependence of the formation rate of nitrophenols versus the product [Phenol] $I_{abs}^{NO_2^-}$. The following equations can be obtained:

$$\frac{d[2-NP]}{dt} = 50.0 \cdot [Phenol] \cdot I_{abs}^{NO_2^-}$$

$$\frac{d[4-NP]}{dt} = 30.9 \cdot [Phenol] \cdot I_{abs}^{NO_2^-}$$

The numerical coefficients would be constant at constant bicarbonate. The dependence on bicarbonate concentration of the initial formation rates of nitrophenols is discussed in the manuscript.

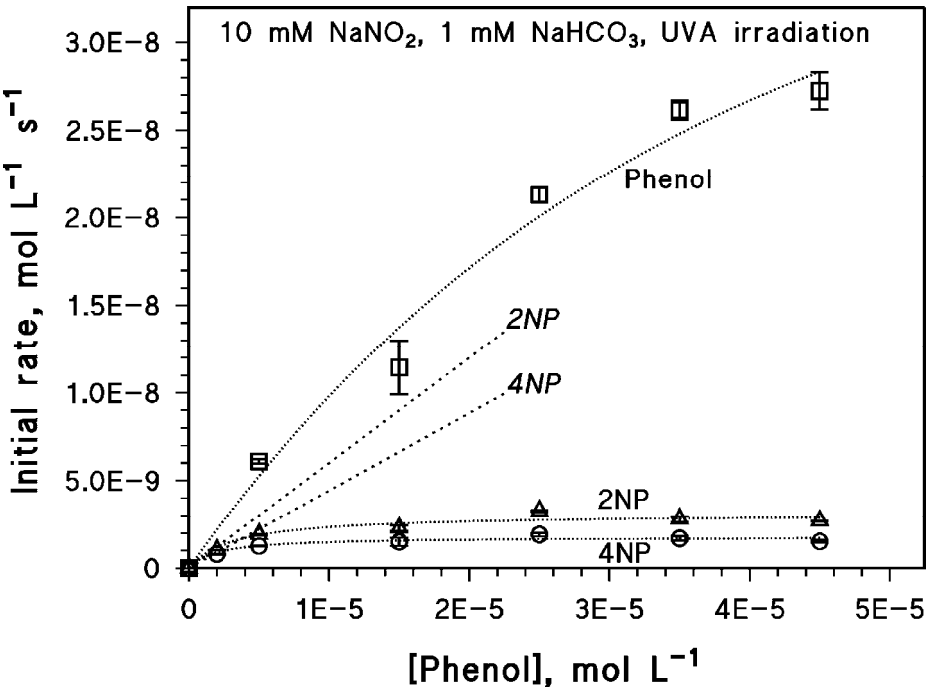

Figure S13. Initial rates of phenol transformation and nitrophenol formation upon UVA irradiation of 10 mM $NaNO_2$ and 1 mM $NaHCO_3$, as a function of phenol concentration. The tangents to the nitrophenol curves at [Phenol] = 0 are also shown on the graph.

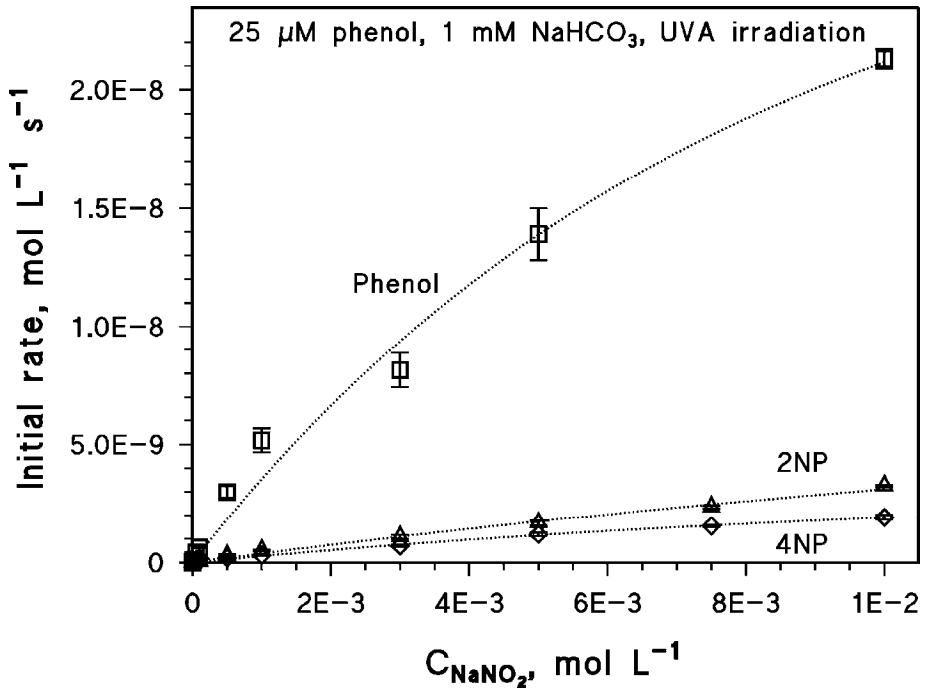

Figure S14. Initial rates of phenol transformation and nitrophenol formation upon UVA irradiation of 25 μM phenol and 1 mM $NaHCO_3$, as a function of nitrite concentration. The connecting curves are just a guide for the eye.

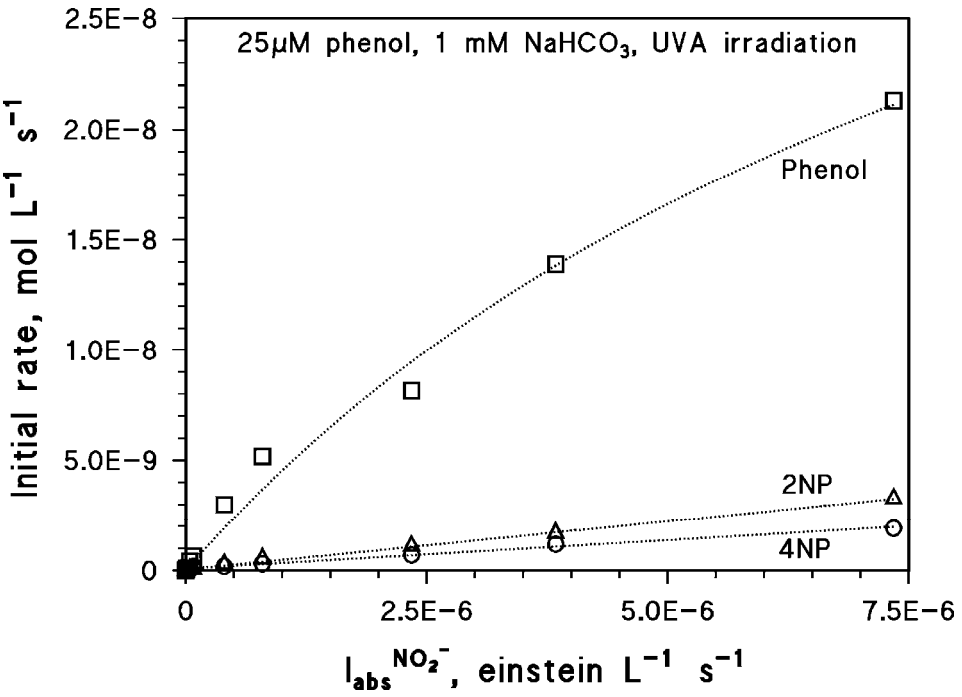

Figure S15. Dependence on $I_{abs}^{NO_2^-}$ of the initial rates of phenol transformation and nitrophenol formation upon UVA irradiation of 25 μM phenol and 1 mM $NaHCO_3$. The phenol curve is just a guide for the eye; nitrophenol formation data have been fitted with linear functions, with very good agreement.